# Genotoxic Damage Activates the AMPK-1 Isoform in the Nucleus via Ca2+/CaMKK2 Signaling to Enhance Tumor Cell Survival

# DNA damage by etoposide activates the α1 isoform of AMP-activated protein kinase in the nucleus via the $Ca^{2+}$/CaMKK2 pathway, enhancing human tumor cell survival

[1]Diana Vara-Ciruelos*, [1]Madhumita Dandapani*, [1]Alexander Gray, [2]Ejaife O. Agbani, [2]A. Mark Evans and [1]D. Grahame Hardie**

[1]Division of Cell Signalling & Immunology, College of Life Sciences, University of Dundee, Dow Street, Dundee, DD1 5EH, Scotland, UK

[2]Centre for Integrative Physiology, University of Edinburgh, Hugh Robson Building, George Square, Edinburgh EH8 9XD, Scotland, UK

**Corresponding author: Prof. D.G. Hardie, Division of Cell Signalling & Immunology, College of Life Sciences, University of Dundee, Dow Street, Dundee, DD1 5EH, Scotland, UK; e-mail: d.g.hardie@dundee.ac.uk; Tel: +44 (1382) 384253

*joint first authors

Running title: Activation of AMPK by etoposide enhances cell survival

Keywords: AMP-activated protein kinase; CaMKK2; DNA damage; etoposide; cell survival

Length of main text: 5,907 words

Number of Figures: 7

Number of Tables: 0

The authors declare no potential conflicts of interest.

DVC was supported by a Programme Grant (C37030/A15101) awarded to DGH by Cancer Research UK, MD by a Clinical PhD studentship from the Wellcome Trust, and AG by a Senior Investigator Award (097726) to DGH by the Wellcome Trust. DGH was also indirectly supported by the pharmaceutical companies supporting the Division of Signal Transduction Therapy at Dundee (Boehringer-Ingelheim, GlaxoSmithKline and Merck KgaA). OAE and AME were supported by a Programme Grant (081195) from the Wellcome Trust.

## Abstract

Many genotoxic cancer treatments activate AMPK, but the mechanisms of AMPK activation in response to DNA damage, and its downstream consequences, have been unclear. We report that etoposide treatment of cells activates the α1 but not the α2 isoform of AMPK, primarily within the nucleus. AMPK activation is independent of the DNA damage-activated kinase ATM, and of the principal upstream kinase for AMPK, LKB1, but correlates with increased nuclear $Ca^{2+}$ and requires the $Ca^{2+}$/calmodulin-dependent kinase, CaMKK2. Intriguingly, $Ca^{2+}$-dependent activation of AMPK in two different LKB1-null cancer cell lines caused G1 cell cycle arrest, and enhanced cell viability/survival after etoposide treatment, with both effects being abolished by knockout of AMPK-α1 and -α2. The CDK4/CDK6 inhibitor palbociclib also caused G1 arrest in G361 but not HeLa cells and, consistent with this, enhanced cell survival after etoposide treatment only in G361 cells. These results suggest that AMPK activation protects cells against etoposide by limiting entry into S phase, where they would be more vulnerable to genotoxic stress.


## Implications

Our results suggest that the α1 isoform of AMPK promotes tumorigenesis by protecting cells against genotoxic stress, which may explain findings that the gene encoding AMPK- α1 (but not - α2) is amplified in some human cancers. They also suggest that α1-selective inhibitors might enhance anti-cancer effects of genotoxic treatments such as etoposide.

## Introduction

The wild mandrake or May Apple *(Podophyllum peltatum),* which was used in traditional native American medicine, contains the natural product podophyllotoxin (1). Podophyllotoxin itself proved to be too toxic for human use, but the synthetic derivative etoposide (also known as VP-16) was approved for cancer treatment in 1983. Etoposide acts by binding to topoisomerase II (2), an enzyme that can relax DNA supercoiling, insert or remove knots, and catenate or decatenate DNA. It catalyzes an ATP-dependent cycle in which both strands of one DNA helix are broken, followed by passage through this break of a second helix and religation of the breaks in the first. By inhibiting the religation step,

etoposide and other anti-cancer agents such as doxorubicin create double-strand breaks. They can also cause trapping of complexes in which tyrosine residues of the topoisomerase II homodimer remain covalently attached to phosphate groups of the nucleotide at the 5' end of a DNA break, interfering with subsequent DNA replication and transcription (3). Since topoisomerase II function is particularly crucial during S phase when DNA is being replicated, rapidly proliferating cells (including tumor cells) are more susceptible to cell death induced by etoposide than quiescent cells.

The AMP-activated protein kinase (AMPK) is a sensor of cellular energy status expressed in essentially all eukaryotic cells, which occurs universally as heterotrimeric complexes comprising catalytic α subunits and regulatory β and γ subunits (4-6). AMPK is activated by phosphorylation of a conserved threonine residue within the activation loop of the kinase domain on the α subunit, usually referred to as Thr172. Thr172 is phosphorylated in vivo by a complex containing the tumor suppressor kinase LKB1, or by $Ca^{2+}$/calmodulin-dependent protein kinase kinases (CaMKKs), especially CaMKK2 (4-6). The LKB1 complex appears to be constitutively active, but displacement of ATP by AMP at two or more sites on the regulatory γ subunit of AMPK leads to increased net Thr172 phosphorylation. This occurs because AMP binding triggers conformational changes that promote Thr172 phosphorylation by LKB1 and inhibit Thr172 dephosphorylation by protein phosphatases, with these effects being mimicked by ADP (7, 8); binding of AMP (but not ADP) also causes further allosteric activation (9). Because increases in the cellular ADP:ATP ratio (signifying energy deficit) are always accompanied by even larger increases in the AMP:ATP ratio, these three effects allow AMPK to act as an ultrasensitive sensor of cellular energy status. The CaMKK2-AMPK pathway appears to be activated solely by increases in intracellular $Ca^{2+}$, which can be caused by addition to cells of $Ca^{2+}$ ionophores such as A23187, or by hormones or cytokines that increase intracellular $Ca^{2+}$ (4-6).

Each AMPK subunit exists as multiple isoforms (α1/α2, β1/β2, γ1/γ2/γ3) encoded by multiple genes *(PRKAA1/2, PRKAB1/2, PRKAG1/2/3)*. Intriguingly, while the *PRKAA2* gene (encoding α2) is quite often mutated in human cancers, consistent with the idea that it helps to exert the tumor suppressor role of LKB1, the *PRKAA1* and *PRKAB2* genes (encoding α1 and β2) are frequently amplified instead, suggesting that their amplification may be selected for because they promote tumor formation (5, 10).

The reason for the distinct behaviors of these AMPK-encoding genes in human cancers has been unclear.

Fu et al (11) reported that etoposide activated AMPK, and claimed that the effect was dependent on the protein kinase ataxia-telangiectasia mutated (ATM), because it appeared to be absent in ATM-deficient cells. ATM is a member of the phosphatidylinositol 3-kinase-like kinase (PIKK) family, with the genetic disorder ataxia-telangiectasia being caused by loss-of-function mutations in the *ATM* gene. ATM is activated in normal cells by double strand breaks in DNA, such as those induced by etoposide. Once activated, ATM autophosphorylates on Ser1981, and phosphorylates downstream targets such as the histone variant, H2AX, and Structural Maintenance of Chromosomes Protein-1 (SMC1); these events can be used as biomarkers both for ATM activation and for DNA damage (12). ATM also phosphorylates LKB1 at Thr366 (13), and it was reported that activation of AMPK by etoposide in prostate cancer cells was reduced by shRNA-mediated knockdown of either ATM or LKB1 (14), suggesting the existence of a kinase cascade from ATM to LKB1 to AMPK. Arguing against this, however, etoposide still activated AMPK in the LKB1-null HeLa cell line (11), while ionizing radiation (which causes double stranded DNA breaks and also activates ATM) activates AMPK in another LKB1-null tumor line, A549 cells (15).

To address these discrepancies, we investigated the mechanism by which etoposide activates AMPK. We show that activation of AMPK is restricted to the α1 isoform within the nucleus, and does not require ATM or LKB1 but is dependent on CaMKK2 and triggered by increases in nuclear $Ca^{2+}$. We also show that prior activation of either isoform enhances cell survival during etoposide treatment. These results not only provide a potential explanation for the findings that the gene encoding AMPK-α1 (but not –α2) is amplified in some human cancers, but also suggest that pharmacological inhibitors of AMPK might make tumor cells more sensitive to death induced by DNA-damaging treatments, and might therefore be useful adjuncts to chemotherapy or radiotherapy. If these inhibitors were α1-selective, this might avoid potential systemic side effects caused by inhibition of α2 complexes.

# Material and Methods

## Materials

A23187, nocodazole, propidium iodide , etoposide, palbociclib, STO609 and KU-5593 were from Sigma-Aldrich. Antibodies against actin (A5441) were from Sigma-Aldrich, against p-AMPK (pT172; A2535), p-ATM (pS1981; 4526) and total ATM (2631) were from Cell Signaling, against phospho-SMC1 (S966-P; A300-050A) and total SMC1 (A300-055A) were from Bethyl labs. Antibodies against AMPK-α1 and -α2, the phosphorylated form of acetyl-CoA carboxylase (pACC) and total ACC have been described previously (16, 17). Secondary antibodies were from Li-Cor Biosciences.

## Cell culture

All cell lines were from the European Collection of Authenticated Cell Cultures (ECACC), except immortalized mouse embryo fibroblasts (MEFS), which were a gift from Dr Benoit Viollet, INSERM, Paris (18). HeLa and G361 cells were re-validated during the project by STR profiling (Public Health England, certificate dated 08/14/2015); HEK-293 cells used in Fig. 2C and Supplementary Fig. S2 were purchased from ECACC in January 2016. G361 cells were cultured in McCoy's 5A medium containing 1% (v/v) glutamine, 10% (v/v) fetal bovine serum (FBS) and 1% (v/v) penicillin/streptomycin. HeLa and HEK-293 cells and MEFs were cultured in Dulbecco's Modified Eagle's Medium (DMEM) with 10% (v/v) FBS and 1% (v/v) penicillin/streptomycin.

## AMPK assays

Endogenous AMPK isoforms were assayed by immunoprecipitate kinase assays as described (19, 20) using the *AMARA* peptide (21) as substrate. AMPK-α1 or –α2 were assayed by immunoprecipitation with α1- or α2-specific antibodies, whereas total AMPK was assayed by immunoprecipitation with an equal mixture of α1- and α2-specific antibodies.

## Construction of AMPK knockout cells

Knockout of AMPK-α1 and -α2 (*PRKAA1* and *PRKAA2*) in G361 and HeLa cells was carried out using the CRISPR-Cas9 method, as described previously for G361 cells (22).

## Immunofluorescence microscopy

Cells were grown on glass coverslips in 6 well dishes until 40-80% confluent and then treated with drugs or vehicle control. The coverslips were washed 3x in PBS, fixed in 4% paraformaldehyde in PBS for 20 min, and washed again 3x with PBS. The cells were then permeabilised in 0.2% Triton X-100 in PBS for 5 min, and washed again 3x with PBS. They were then placed in blocking buffer (PBS with 0.2% fish skin gelatin) for 1 hr and stained with primary antibody (1:300- 1:1000 in blocking buffer) for 30 min. After further washing in blocking buffer, the coverslips were incubated with fluorescent secondary antibody (1:200 dilution in blocking buffer) for 30 min. They were then mounted on slides using Vectashield and sealed with nail varnish. The slides were imaged on the Deltavision deconvolution microscope and images acquired and deconvolved using the SoftWorx program.

## Live cell imaging with Fluo4

Cells were grown on glass bottom dishes (Willco Wells) until 40-80% confluent. They were then loaded with Fluo4-AM dye (1 μM) plus Hoechst 33342 for 20-30 min. The cells were then washed with PBS and fresh medium added. The Willco dish was mounted onto a stage pre-heated to 37$^{o}$C and enclosed with a lid to deliver 5% $CO_2$ to the cells. Calcium flux was measured using the DeltaVision OMX system with fluorescence measured at 488 nm using a 63x objective. Image analysis and quantification was performed using ImageJ software.

## siRNA knockdown of CaMKK2

Reverse transfection of siRNA constructs against CaMKK2 were carried out according to protocols detailed in the Ambion™ siRNA starter kit. Briefly, transfection reagent (siPORT) was diluted 1 in 20 in Opti-MEM medium and allowed to incubate for 10 min. Meanwhile, cells were trypsinised for 5 minutes and the trypsin quenched with complete media. siRNA (Ambion, Life Technologies) was diluted in Opti-MEM to a final concentration of 5 nM. siRNA and diluted transfection reagent were then mixed and incubated for 10 min. The siRNA- siPORT mixture was added to 6 well plates and cells were seeded into the 6 well plates. The plates were returned to the incubator for 24 hr, after which treatment with vehicle or drugs was carried out. Knockdown was confirmed by Western blotting.

## Clonogenic and MTT survival assays

For clonogenic survival assays, cells were seeded into 6 well plates at equal density and treated at 40-80% confluence with vehicle control or different concentrations of drug for 24 hr. Cells were trypsinized in 0.5 ml of trypsin:EDTA for 5 min and then diluted with 1 ml of complete medium. The cells in the control flask were counted using a hemocytometer under a microscope and 2000 cells seeded in triplicate into 10 cm dishes containing 10 ml of medium. The same volume of cell suspension was aspirated from the treated flasks and seeded in triplicate into 10 cm dishes also containing 10 ml of medium. The dishes were placed at 37 ºC in an incubator for 10-15 days. On last day, the medium was aspirated; the cells were fixed with ice-cold methanol for 10 min and stained with 0.3% w/v methylene blue in methanol for 10 min. The dishes were washed with de-ionised water and the number of colonies counted manually.

For MTT assays, cells were seeded in 12 well plates until 40-80% confluence and treated for 48 hr. The cells were then incubated with 0.5% of 3-(4,5-dimethyl-2-thiazolyl)-2,5-diphenyl-2H-tetrazolium bromide (MTT) for 3 hr. The growth medium was aspirated off and formazan crystals were dissolved in 500 µl of acidified isopropanol. The intensity was measured by spectrophotometry at 570 nm.

## Cell cycle analysis

Cells were seeded in 6 cm dishes until 40-80% confluence and treated for 16-18 hr. Cells were trypsinized and the cells were pelleted, transferred into 5 ml Falcon tubes and washed with PBS containing 1% fetal calf serum and 0.1 mM EDTA. The cells were then fixed with ice-cold 70% ethanol for >2 hr. The cells were washed twice in the PBS buffer and stained with propidium iodide (diluted 1 in 20 in the PBS buffer) with RNAse added to digest RNA. Cell cycle analysis was performed on the Calibur flow cytometer and analysis performed using Flow Jo software.

## Additional analytical procedures

SDS-PAGE was performed using precast Bis-Tris 4–12% gradient polyacrylamide gels in the MOPS buffer system (Invitrogen). Proteins were transferred to nitrocellulose membranes (BioRad) using the Xcell II Blot Module (Invitrogen). Membranes were blocked for 1 hr in Tris-buffered saline (TBS) containing 5% (w/v) non-fat dried skimmed milk. The membranes were probed with appropriate

antibody (0.1–1 μg/ml) in TBS-Tween and 2% (w/v) non-fat dried skimmed milk. Detection was performed using secondary antibody (1 μg/ml) coupled to IR 680 or IR 800 dye, and the membranes scanned using the Li-Cor Odyssey IR imager.

### Presentation of data and statistical analysis

Significances of differences were estimated using GraphPad Prism 6 for Mac OSX, using Student's t test, 1-way or 2-way ANOVA as appropriate. Unless stated otherwise, Sidak's multiple comparison test was used for post-hoc analysis. Numbers of replicates (n) refer to biological replicates, i.e. the number of independent cell cultures analyzed. Significance of differences are indicated as follows: *P<0.05, **P<0.01, ***P<0.001, ****P<0.0001 or †P<0.05, ††P<0.01, †††P<0.001, ††††P<0.0001; ns, not significant.

## Results

### AMPK activation by etoposide does not require LKB1

We initially studied the effects of etoposide in cell lines expressing LKB1, including the human embryonic kidney cell line, HEK-293. Surprisingly, we could not detect significant AMPK activation in these cells using kinase assays, although it could be readily observed in two LKB1-null tumor cell lines, i.e. HeLa (cervical cancer) and G361 (melanoma) cells. We could also observe AMPK activation in immortalized mouse embryo fibroblasts (MEFs), which do express LKB1 (Fig. 1A).

In HeLa cells, AMPK activation following addition of 30 μM etoposide was quite slow and relatively modest in extent, becoming significant by 6-9 hours and reaching a maximum of 2- to 3-fold after 18 hours (see Fig. 5A). Infusion of high-dose etoposide in humans results in peak plasma concentrations ranging from 50-200 μM (23), and AMPK activation after 16 hr treatment of HeLa cells occurred at etoposide concentrations from 30 to 300 μM (Fig. 1B). AMPK activation was associated with increased Thr172 phosphorylation, by 1.8 ± 0.3-fold (n.s.), 2.2 ± 0.3-fold ($P$ <0.05) and 2.3 ± 0.3-fold (P <0.05) at 30, 100 and 300 μM etoposide respectively (mean ± SEM, n = 6), and with phosphorylation of the ATM substrate SMC1, although phosphorylation of the latter appeared to be saturated at 30 μM (Fig. 1B). As expected, activation and Thr172 phosphorylation of AMPK was also

observed following treatment of HeLa cells with the $Ca^{2+}$ ionophore A23187 (which activates the upstream kinase CaMKK2) although the degree of activation was larger than that obtained with etoposide. However, A23187 treatment did not lead to phosphorylation of SMC1, suggesting that ATM was not activated by increasing cellular $Ca^{2+}$ (Fig. 1B). Very similar effects of etoposide and A23187 were observed in G361 cells (Fig. 1C), where the effects of etoposide on Thr172 phosphorylation were 2.1 ± 0.1-fold (n.s.), 3.5 ± 0.4-fold ($P$ <0.001) and 3.7 ± 0.5-fold (P <0.001) at 30, 100 and 300 μM respectively (mean ± SEM, n = 4).

## AMPK activation by etoposide occurs primarily within the nucleus

Fig. 2A shows fluorescence micrographs of HeLa cells treated with vehicle (DMSO), etoposide (100 μM) or A23187. The cells were fixed and labeled with antibodies recognizing ATM phosphorylated at Ser1981 (pATM) or AMPK phosphorylated at Thr172 (pT172). Quantification of the nuclear and cytoplasmic fluorescence is shown in Fig. 2B, left-hand panels (n = 10). As expected, large increases (13-fold) in nuclear staining were obtained with the anti-pATM antibody after treatment with etoposide, but not A23187. By contrast, large increases in nuclear staining were obtained with anti-pT172 antibody after treatment with either etoposide (13-fold) or A23187 (9-fold). Although A23187 also appeared to increase cytoplasmic pT172 staining in HeLa cells, this was not statistically significant. Similar results were obtained with G361 cells, although in these cells A23187 did cause a significant increase in cytoplasmic pT172 staining (Supplementary Fig. S1; quantification in Fig, 2C, right). These results show that etoposide activates AMPK primarily in the nucleus, in both HeLa and G361 cells.

Using the anti-pT172 antibody to detect AMPK activation in HeLa cells, fluorescence could be observed in most nuclei after treatment for 18 hr with 100 μM etoposide, but was still observed in some nuclei even at much lower etoposide concentrations (250 nM, Supplementary Fig. S2, arrows); these invariably corresponded with nuclei that were also positive for pATM, indicating the occurrence of DNA damage.

Because basal Thr172 phosphorylation and AMPK activity is much higher in the cytoplasm of cells that express LKB1 such as HEK-293 cells (24), we hypothesized that this might have been masking

changes in the small pool of AMPK in the nucleus, explaining why we had not been able to initially detect effects of etoposide in HEK-293 cells. Consistent with this, in control HEK-293 cells treated with DMSO for 18 hr there was a diffuse cytoplasmic and nuclear fluorescence detected using anti-pT172 antibodies, such that it was difficult to distinguish the two compartments. Most cells also displayed at least one perinuclear patch with more intense fluorescence; these appear to represent the Golgi apparatus, since they stained with antibodies against the Golgi maker, GM130 (data not shown). In cells treated with low etoposide concentrations (3 μM) the nuclei were more fluorescent than the cytoplasm in some cells, once again corresponding with cells where the signal for nuclear pATM was increased (Supplementary Fig. S3, arrows). Fig. 2C shows quantification of results from a large number of cells (n = 18). The mean absolute fluorescence appeared to increase in response to etoposide in the nucleus and decrease in the cytoplasm, while remaining constant when averaged across the whole cell, although these effects were not statistically significant (left-hand panel). However, when the results were expressed as nuclear:cytoplasmic ratios there was a significant increase in response to 3 μM etoposide (right-hand panel). Thus, etoposide appears to activate AMPK within the nuclei of HEK-293 cells, although this is difficult to detect because it can be masked by the high basal activity in the larger pool of AMPK in the cytoplasm.

## AMPK activation by etoposide is specific for the α1 isoform

Because the sequences around Thr172 are identical in α1 and α2, the anti-pT172 antibody does not distinguish the two AMPK catalytic subunit isoforms. However, human α1 (predicted mass 64,009 Da) is slightly larger than α2 (62,319 Da), and the two isoforms can be resolved by SDS-PAGE. In Fig. 3A we analyzed lysates from triplicate dishes of control and etoposide-treated HeLa cells by dual label Western blotting using anti-pT172 antibodies labeled with IRDye 680 (red), and either α1- or α2-specific antibodies labeled with IRDye800 (green). In the upper blot (probed with anti-pT172 and anti-α1) a single band appears predominantly green in the control lanes but becomes more yellow (indicating increased Thr172 phosphorylation) after etoposide treatment. In the lower blot (probed with anti-pT172 and anti-α2) two bands are evident, an upper red band (α1) that becomes more intense after etoposide treatment, and a lower green band (α2) whose intensity or color does not change. The

intensity in the pT172 (red) channel for α1 increased by 2.1 ± 0.1-fold ($P < 0.0001$, $n = 3$) and 2.0 ± 0.1-fold ($P = 0.0001$, $n = 3$) in the upper and lower panels respectively, but was unchanged for α2. These results show that Thr172 phosphorylation in response to etoposide occurs exclusively with the α1 isoform. To confirm this, we immunoprecipitated complexes from cell lysates of HeLa, G361 and A549 cells using α1- or α2-specific antibodies, and measured kinase activity. The results (Fig. 3B-D) showed that 30-300 μM etoposide caused progressive activation of α1 complexes in all three cell types. In HeLa and A549 cells etoposide failed to activate α2 complexes (Figs. 3B, 3D), while in G361 cells the activity of α2 complexes was too low to measure reliably (Fig. 3C). As a positive control, the $Ca^{2+}$ ionophore A23187 markedly activated both α1 and α2 complexes in HeLa and A549 cells, and α1 complexes in G361 cells. We also performed Western blots in A549 cells (Fig. 3E), which showed, similar to the results in HeLa and G361 cells (Figs. 1B/1C), that pSMC1 phosphorylation was increased by etoposide but not A231787, whereas there were small increases in Thr172 phosphorylation in response to etoposide and a larger increase in response to A23187, correlating with the changes in AMPK activity. Interestingly, phosphorylation of the downstream target of AMPK, acetyl-CoA carboxylase (ACC), did not appear to increase in response to etoposide, although it clearly increased in response to A23187 (Fig. 3E).

## AMPK activation by etoposide requires CaMKK2 but not ATM

Since AMPK activation by etoposide in HeLa, G361 and A549 cells occurs in the absence of LKB1, we examined whether it required the other well-established upstream kinase for AMPK, CaMKK2. Fig. 4A shows that the CaMKK2 inhibitor STO609 had no effect on etoposide-induced phosphorylation of SMC1 (which is catalyzed by ATM), but did inhibit basal AMPK activity and Thr172 phosphorylation, as well as the increases induced by etoposide (although at the concentration used it did not block the effects of etoposide completely). Fig. 4A shows that (as in A549 cells, Fig. 3E), etoposide did not increase phosphorylation of the classical AMPK target acetyl-CoA carboxylase (ACC), although in other experiments (Fig. 4C) it was phosphorylated in response to A23187. Since STO-609 is not completely selective for CaMKK2 (17), we also assessed the requirement for CaMKK2 via siRNA knockdown. Western blots show that we obtained effective CaMKK2 knockdown that blocked AMPK

activation and Thr172 phosphorylation in response to both etoposide (Fig. 4B) and A23187 (Fig. 4C). As expected, CaMKK2 knockdown did not affect etoposide-induced phosphorylation of the ATM target SMC1 (Fig. 4B), although it prevented phosphorylation of ACC in response to A23187 (Fig. 4C).

To examine the involvement of ATM, we used the ATM-selective inhibitor KU-55933 (25). As expected, KU-55933 blocked the phosphorylation of the ATM target SMC1 in response to etoposide. However, although it appeared to cause a modest reduction in basal activity and Thr172 phosphorylation of AMPK, it did not prevent the increased AMPK activity and Thr172 phosphorylation caused by etoposide (Fig. 4D). Thus, in these cells the regulation of AMPK by etoposide is ATM-independent.

## AMPK activation is associated with increases in nuclear [$Ca^{2+}$]

Since activation and Thr172 phosphorylation of AMPK in response to etoposide required CaMKK2, we suspected that it might be associated with increases in nuclear $Ca^{2+}$ concentration. Fig. 5A shows a time course of AMPK activation after addition of etoposide in HeLa cells. After a lag of around 3 hours, AMPK activation became evident by 6 hours and increased further up to 18 hours. We used the $Ca^{2+}$-sensitive dye fluo-4, administered to cells in the form of the acetoxymethyl ester fluo-4 AM, to estimate changes in $Ca^{2+}$ within the nucleus and cytoplasm at 3 hr intervals. The ratio of fluorescence at the time of measurement and at time zero ($F/F_0$), was used as an index of [$Ca^{2+}$]. Interestingly, slow, progressive increases in nuclear [$Ca^{2+}$] were observed which followed a similar time course to changes in AMPK activity, becoming significant at 6 hours and continuing to increase up to about 18 hours. Cytoplasmic $Ca^{2+}$ did not exhibit such significant changes over the same time points (Fig. 5B).

## A23187 enhances cell survival during etoposide treatment via AMPK activation

Using the CRISPR-Cas9 system, we generated HeLa and G361 cells with single (α1KO or α2KO) or double (DKO) knockouts of the AMPK catalytic subunits. Fig. 6A shows that α1 and/or α2 were absent from the knockout HeLa cells as expected. Interestingly, α2 expression was markedly up-regulated in α1KO HeLa cells. We were unable to detect α2 by Western blotting in the G361 cells (Fig. 6B), consistent with our failure to detect it using kinase assays (see above). Also consistent with

this, phosphorylation of the AMPK target ACC in response to the AMPK activator $H_2O_2$ (26) was abolished in G361 cells by knockout of α1 only, although in HeLa cells this required knockout of both α1 and α2 (Fig. 6A/B).

We next used two types of cell survival assay to assess the effect of prior AMPK activation by A23187 on cell death induced by etoposide treatment of HeLa cells. Using MTT assays and treatment for 48 hours (Fig. 6C), 10 or 30 μM etoposide reduced cell survival to 21% and 7% of the DMSO control, respectively. However, prior treatment with A23187 for 6 hours to activate AMPK significantly enhanced cell survival to 47% and 14% of control, respectively. Similar protective effects of A23187 were seen in α1KO and α2KO cells although the basal levels of survival appeared to be slightly higher in these cells. However, the protective effect of A23187 treatment was completely abolished in DKO cells at both etoposide concentrations. Similar results were obtained using the more sensitive clonogenic survival assays (Fig. 6D), although much lower concentrations of etoposide (100 and 250 nM) and shorter incubation times (18 hours) were used in these assays. One other difference was that clonogenic survival was significantly lower in DKO cells at both 100 and 250 nM etoposide even in cells not treated with A23187, an effect not seen using the MTT assays. Fig. 6E confirms using anti-pSMC1 blots that ATM was activated to a similar extent at all four concentrations of etoposide used in Figs. 6C and 6D, and that this was unaffected by single or double knockouts of the two AMPK catalytic subunit isoforms.

We suspected that the protection against cell death provided by AMPK activation might be due to G1 cell cycle arrest, which would reduce entry of cells into S phase where they would be more vulnerable to DNA damage induced by etoposide. To confirm that A23187 induced G1 arrest in HeLa cells, we treated them with or without A23187 in the presence of nocodazole (which prevents cells that have already traversed the G1:S boundary from progressing through into the subsequent G1 phase). Fig. 6F shows that A23187 caused a >10-fold increase in G1:G2 ratio in WT cells, as expected for an agent causing G1 arrest. Similar results were obtained in α1KO or α2KO cells, showing that either isoform is capable of causing cell cycle arrest. However, a significant increase in G1:G2 ratio was not observed in DKO cells.

### Other treatments causing G1 arrest provided similar protection against etoposide

To test whether other treatments that caused G1 arrest would provide protection against etoposide-induced cell death, we initially used palbociclib (PBC, also known as PD332991), an inhibitor of the cyclin-dependent kinases CDK4/CDK6 (27, 28). Interestingly, PBC did not cause cell cycle arrest in HeLa cells (Fig. 7A). However, in G361 cells PBC from 0.1 to 10 nM caused a progressive increase in the proportion of G361 cells in G1 phase, with corresponding decreases in the proportions in S and G2/M phases (Fig. 7B). Tellingly, PBC did not protect against cell death induced by etoposide in clonogenic survival assays in HeLa cells (Fig. 7C), but provided marked protection in G361 cells (Fig. 7D). We have shown previously that A23187 treatment of G361 cells causes a G1 arrest that is abolished in AMPK DKO cells (22). Supplementary Fig. S4 confirms that, similar to HeLa cells, prior treatment with A23187 protected G361 cells against cell death induced by etoposide in clonogenic survival assays, with the effect being abolished in DKO cells.

To confirm that another agent that caused cell cycle arrest would protect HeLa cells against etoposide, we used aphidicolin, which causes arrest in early S phase by inhibiting DNA polymerase-α (29). Unlike palbociclib, aphidicolin cause a marked arrest at the G1/S boundary (Fig. 7E) and also provided significant protection against cell death induced by etoposide in clonogenic survival assays (Fig. 7F).

## Discussion

We have confirmed that the DNA-damaging agent etoposide activates AMPK in several different cell lines as reported previously (11, 14), but also present new findings that AMPK activation by etoposide occurs primarily in the nucleus, and is specific for complexes containing the α1 isoform of the catalytic subunit even when α2 was also expressed, as in HeLa and A549 cells. Since these cells do not express LKB1, our results rule out a role for that kinase. We show instead that the effect is catalyzed by the alternate upstream kinase CaMKK2, since it was reduced either by the CaMKK inhibitor STO-609, or by knocking down CaMKK2 using siRNA. The correlation between AMPK activation and nuclear $[Ca^{2+}]$ (Fig. 5) suggests that activation of AMPK by etoposide may be mediated by increases in nuclear $[Ca^{2+}]$ rather than any intrinsic change in CaMKK2 activity, although the source of the increased

371 nuclear $Ca^{2+}$, and the mechanism by which it is released in response to etoposide and/or DNA damage,
372 remains unclear.

373 We were initially unable to detect significant Thr172 phosphorylation or activation of AMPK by
374 etoposide in HEK-293 cells, which express normal levels of LKB1. However, we subsequently
375 observed increased Thr172 phosphorylation in the nuclei of HEK-293 cells by immunofluorescence
376 microscopy. We believe that we could not detect changes in global Thr172 phosphorylation or AMPK
377 activation in these cells because the high basal levels of these parameters in the cytoplasm (due to the
378 high basal activity of LKB1) were obscuring changes in the small pool of AMPK within the nucleus.

379 It was previously reported that AMPK activation by etoposide in a prostate cancer cell line (C4-2)
380 was reduced by knocking down ATM or LKB1 using RNAi (14). Since ATM had been previously
381 shown to phosphorylate LKB1 at Thr366 (13), it was proposed (14) that there was a kinase cascade
382 from ATM to LKB1 to AMPK. However, Thr366 phosphorylation has been reported to have no effect
383 on either the activity or the localization of LKB1 in G361 cells (13). Moreover, this mechanism cannot
384 explain the effects in the cells we studied because: (i) in HeLa cells, etoposide activated AMPK via a
385 mechanism that required CaMKK2, but not LKB1; (ii) although etoposide activated ATM in HeLa
386 cells, the ATM inhibitor KU-55933 did not prevent increased AMPK activity and Thr172
387 phosphorylation in response to etoposide, despite blocking phosphorylation of a known ATM target,
388 SMC1.

389 One interesting question raised by our study is why AMPK activation by etoposide is restricted to
390 nuclear $\alpha$1 complexes. LKB1 is only catalytically active when it forms a complex with the accessory
391 subunits STRAD and MO25 (30), and association with these subunits causes its exclusion from the
392 nucleus (31), implying that LKB1 may only be able to activate cytoplasmic AMPK. Consistent with
393 this, using a FRET-based reporter that can monitor AMPK activity in real time in single cells (32),
394 AMPK activation by 2-deoxyglucose [an inhibitor of glycolysis that activates AMPK by increasing
395 cellular AMP, and is therefore LKB1-dependent (33)] occurred only in the cytoplasm, whereas
396 activation by A23187 [a $Ca^{2+}$ ionophore that works via the $Ca^{2+}$/CaMKK2 pathway independently of
397 AMP (33)] occurred initially in the cytoplasm and then in the nucleus. These results suggest that
398 CaMKK2 must be present in the nucleus, since if the effect was due to translocation of activated

AMPK, it should work equally well after treatment with 2-deoxyglucose or A23187. There is also evidence that α2-containing complexes are activated primarily by the AMP- and LKB1-dependent mechanism rather than the $Ca^{2+}$/CaMKK2 mechanism *in vivo*. For example, conditional LKB1 knockout in skeletal and cardiac muscle prevented activation of α2-containing complexes in response to contraction in skeletal muscle or ischemia in cardiac muscle, while having little or no effect on the activity of α1-containing complexes (34, 35). The reasons for this apparent selectivity of upstream kinases for α1 or α2-containing complexes *in vivo* remain unclear, because the LKB1:STRAD:MO25 complex (24) and CaMKK2 (36) phosphorylate and activate both α1- or α2-containing complexes in cell-free assays, while treatment with the $Ca^{2+}$ ionophore A23187 can activate α2 complexes in intact cells (Fig. 2B). One possibility is that this isoform selectivity is due to different subcellular locations of the upstream kinases and the AMPK complexes containing the different α isoforms. Both α1 and α2 contain well-defined nuclear export sequences (37), while nuclear localization sequences are less well-defined, although a short conserved basic sequence in α2 (also present in α1) has been proposed to fulfill that role (38). If α1 complexes were more abundant than α2 complexes in the nuclei of unstimulated HeLa or G361 cells, this might explain why only the former were activated by etoposide. Arguing against this possibility, however, is evidence that it is α2 rather than α1 that is enriched in the nucleus (39), although that was obtained using different cell types. Interestingly, etoposide treatment did not cause phosphorylation of ACC at the AMPK site Ser79, unlike A23187 (Figs. 3E, 4A, 4C). ACC phosphorylation is a universally used biomarker for AMPK activation, and etoposide is the first AMPK activator we have studied that does not trigger it. The obvious explanation is that etoposide activates AMPK primarily in the nucleus, from which ACC (a large cytoplasmic protein) is excluded.

Another novel finding in our study was that prior elevation of intracellular $Ca^{2+}$ for 6 hours using the $Ca^{2+}$ ionophore A23187 protected against cell death induced by etoposide, both in short-term MTT assays and in clonogenic survival assays. In both cases, the effect was AMPK-dependent, because it was eliminated in HeLa and G361 cells when both catalytic subunit isoforms (α1 and α2) were knocked out using the CRISPR-Cas9 system. Single knockouts did not abolish the effect in HeLa cells, suggesting that either isoform is capable of exerting the protective effect, although we have found that only α1 complexes are activated by etoposide. A caveat here, however, is that knockout of AMPK-α1

caused a marked up-regulation of AMPK-α2 expression (Fig. 6A), raising the possibility that over-expressed AMPK-α2 might perform functions that endogenous levels might not. A notable difference between the MTT and the clonogenic survival assays is that effects of etoposide on cell survival were observed in clonogenic assays at much lower concentrations (100-250 nM, as opposed to 10-30 μM for MTT assays). This is a common finding, and may occur because a low level of DNA damage, which may be quite difficult to detect, is nevertheless sufficient to prevent clonal growth of single cells.

These findings to some extent turn the original view on the role of AMPK in cancer on its head. Because AMPK is immediately downstream of, and activated by, the tumor suppressor LKB1, because it inhibits cell growth and proliferation and switches off the growth-promoting target-of-rapamycin complex-1 (TORC1) when activated (5, 40), and because use of the AMPK-activating drug metformin is associated with a lower risk of cancer in diabetics (41), it had been widely assumed that AMPK was a tumor suppressor. Although AMPK may indeed initially suppress the development of rapidly growing tumors and there may therefore be selection pressure for the LKB1-AMPK pathway to be down-regulated (42), complete loss-of-function of AMPK in human cancers appears to be rare. In fact, there is increasing evidence that AMPK can under some circumstances *enhance* the growth of tumor cells, perhaps by protecting solid tumors against the environmental and nutritional stresses that occur before their new blood supply has been fully established (5, 10, 43, 44). For example, a double knockout of α1 and α2 isoforms in immortalized MEFs prevented their growth as xenografts in immunodeficient mice (18). However, while knocking out α2 alone accelerated growth of H-RasV12-transformed MEFs in vivo, knocking out α1 completely prevented growth, suggesting that α1 but not α2 is required for tumor growth in vivo (45). These results are also consistent with results of recent data mining from the human cancer genome projects, which revealed that while the *PRKAA1* gene (encoding α1) is frequently amplified in human cancers (suggesting that this is a genetic change for which positive selection has occurred), the *PRKAA2* gene (encoding α2) undergoes quite frequent mutations instead, more consistent with it being a tumor suppressor (5, 10). The results shown in Fig. 6 provide the novel finding that AMPK activation using A23187 in LKB1-null tumor cells protects them against cell death induced by the DNA damaging agent, etoposide, and that this is abolished in the absence of AMPK. Since etoposide treatment activates AMPK on its own, the presence of AMPK

should be sufficient to protect the cells against etoposide, even in the absence of A23187. This was indeed the case in clonogenic survival assays in HeLa cells, where cell death was enhanced in the DKO cells not treated with A23187 (Fig. 6D). These results suggest that an AMPK inhibitor (particularly if selective for α1 complexes) might be a useful adjunct to treatment with etoposide, and perhaps other cancer therapies that damage DNA, such as doxorubicin or radiotherapy.

What is the mechanism by which AMPK protects tumor cells against the effects of DNA-damaging agents such as etoposide? AMPK activation using the pharmacological activator 5-aminoimidazole-4-carboxamide ribonucleoside (46), or by glucose deprivation or over-expression of a mutant (T172D) AMPK kinase domain (47), causes cell cycle arrest in G1 phase. We have recently confirmed that these effects of AMPK activators, which are associated with increased expression of the cyclin-dependent kinase inhibitor p21 (CDKN1A), are AMPK-dependent since they were abolished by a double knockout of AMPK (22). A cell cycle arrest in G1 phase would limit the entry of cells into S phase, where they are particularly vulnerable to the generation of double-stranded DNA breaks induced by etoposide while DNA is being replicated. Supporting this proposal, palbociclib, a potent and selective inhibitor of the G1 cyclin-dependent kinases CDK4/CDK6 (27, 28), caused G1 arrest in G361 cells while not arresting HeLa cells and, correlating with this, prior treatment of G361 but not HeLa cells with palbociclib provided marked protection against cell death induced by etoposide. By contrast, aphidicolin caused a G1:S phase cycle arrest in HeLa cells and also protected them against cell death induced by etoposide. Sensitivity of different tumor cell lines to palbociclib has been shown to be inversely correlated with the expression of the CDK inhibitor p16 (CDKN2A) (48, 49). This may explain why the effect of the inhibitor differs between these two cell lines, since p16 is expressed at much higher levels in HeLa than in G361 cells (50).

In summary, DNA-damaging treatments such as etoposide (11) and ionizing radiation (15) have been previously reported to activate AMPK, and it was suggested that the effect of etoposide occurred via a kinase cascade from ATM to LKB1 to AMPK (14). However, we show that the effect of etoposide is independent of ATM and LKB1, and involves instead an increase in nuclear $Ca^{2+}$ that causes activation of CaMKK2. AMPK activation is restricted to the α1 isoform and occurs within the nucleus, so that phosphorylation of ACC, the classical marker for AMPK activation, is not observed.

Moreover, prior AMPK activation using A23187 in two different LKB1-null tumor cell lines protects against cell death induced by etoposide, and this was AMPK-dependent because the effect was abolished when both isoforms of AMPK were knocked out. Taken together with findings that AMPK-α1 is required for growth of transformed mouse embryo fibroblasts as tumors in vivo (45), and that the gene encoding AMPK-α1 is frequently amplified in human tumors (5, 10), this suggests that AMPK inhibitors, and particularly selective inhibitors of AMPK-α1, might be useful adjuncts to cytotoxic drugs, and perhaps also radiotherapy, in human cancer.

## References

1. Slevin ML. The clinical pharmacology of etoposide. Cancer. 1991;67:319-29.
2. Hande KR. Etoposide: four decades of development of a topoisomerase II inhibitor. Eur J Cancer. 1998;34:1514-21.
3. Pommier Y, Leo E, Zhang H, Marchand C. DNA topoisomerases and their poisoning by anticancer and antibacterial drugs. Chem Biol. 2010;17:421-33.
4. Carling D. AMPK signalling in health and disease. Curr Opin Cell Biol. 2017;45:31-7.
5. Ross FA, MacKintosh C, Hardie DG. AMP-activated protein kinase: a cellular energy sensor that comes in 12 flavours. FEBS J. 2016;283:2987-3001.
6. Oakhill JS, Scott JW, Kemp BE. AMPK functions as an adenylate charge-regulated protein kinase. Trends Endocrinol Metab. 2012;23:125-32.
7. Oakhill JS, Steel R, Chen ZP, Scott JW, Ling N, Tam S, et al. AMPK is a direct adenylate charge-regulated protein kinase. Science. 2011;332:1433-5.
8. Xiao B, Sanders MJ, Underwood E, Heath R, Mayer FV, Carmena D, et al. Structure of mammalian AMPK and its regulation by ADP. Nature. 2011;472:230-3.
9. Ross FA, Jensen TE, Hardie DG. Differential regulation by AMP and ADP of AMPK complexes containing different gamma subunit isoforms. Biochem J. 2016;473:189-99.
10. Monteverde T, Muthalagu N, Port J, Murphy DJ. Evidence of cancer promoting roles for AMPK and related kinases. FEBS J. 2015;282:4658-71.

11. Fu X, Wan S, Lyu YL, Liu LF, Qi H. Etoposide induces ATM-dependent mitochondrial biogenesis through AMPK activation. PLoS One. 2008;3:e2009.
12. Cremona CA, Behrens A. ATM signalling and cancer. Oncogene. 2014;33:3351-60.
13. Sapkota GP, Deak M, Kieloch A, Morrice N, Goodarzi AA, Smythe C, et al. Ionizing radiation induces ataxia telangiectasia mutated kinase (ATM)-mediated phosphorylation of LKB1/STK11 at Thr-366. Biochem J. 2002;368:507-16.
14. Luo L, Huang W, Tao R, Hu N, Xiao ZX, Luo Z. ATM and LKB1 dependent activation of AMPK sensitizes cancer cells to etoposide-induced apoptosis. Cancer Lett. 2013;328:114-9.
15. Sanli T, Rashid A, Liu C, Harding S, Bristow RG, Cutz JC, et al. Ionizing radiation activates AMP-activated kinase (AMPK): a target for radiosensitization of human cancer cells. Int J Radiat Oncol Biol Phys. 2010;78:221-9.
16. Woods A, Salt I, Scott J, Hardie DG, Carling D. The a1 and a2 isoforms of the AMP-activated protein kinase have similar activities in rat liver but exhibit differences in substrate specificity *in vitro*. FEBS Lett. 1996;397:347-51.
17. Hawley SA, Pan DA, Mustard KJ, Ross L, Bain J, Edelman AM, et al. Calmodulin-dependent protein kinase kinase-beta is an alternative upstream kinase for AMP-activated protein kinase. Cell Metab. 2005;2:9-19.
18. Laderoute KR, Amin K, Calaoagan JM, Knapp M, Le T, Orduna J, et al. 5'-AMP-activated protein kinase (AMPK) is induced by low-oxygen and glucose deprivation conditions found in solid-tumor microenvironments. Mol Cell Biol. 2006;26:5336-47.
19. Hardie DG, Salt IP, Davies SP. Analysis of the role of the AMP-activated protein kinase in the response to cellular stress. Methods Mol Biol. 2000;99:63-75.
20. Towler MC, Fogarty S, Hawley SA, Pan DA, Martin D, Morrice NA, et al. A novel short splice variant of the tumour suppressor LKB1 is required for spermiogenesis. Biochem J. 2008;416:1-14.
21. Dale S, Wilson WA, Edelman AM, Hardie DG. Similar substrate recognition motifs for mammalian AMP-activated protein kinase, higher plant HMG-CoA reductase kinase-A, yeast SNF1, and mammalian calmodulin-dependent protein kinase I. FEBS Lett. 1995;361:191-5.

22. Fogarty S, Ross FA, Vara Ciruelos D, Gray A, Gowans GJ, Hardie DG. AMPK causes cell cycle arrest in LKB1-deficient cells via activation of CAMKK2. Mol Cancer Res. 2016;14:683-95.
23. Hande KR, Wedlund PJ, Noone RM, Wilkinson GR, Greco FA, Wolff SN. Pharmacokinetics of high-dose etoposide (VP-16-213) administered to cancer patients. Cancer Res. 1984;44:379-82.
24. Hawley SA, Boudeau J, Reid JL, Mustard KJ, Udd L, Makela TP, et al. Complexes between the LKB1 tumor suppressor, STRADa/b and MO25a/b are upstream kinases in the AMP-activated protein kinase cascade. J Biol. 2003;2:28.
25. Hickson I, Zhao Y, Richardson CJ, Green SJ, Martin NM, Orr AI, et al. Identification and characterization of a novel and specific inhibitor of the ataxia-telangiectasia mutated kinase ATM. Cancer Res. 2004;64:9152-9.
26. Auciello FR, Ross FA, Ikematsu N, Hardie DG. Oxidative stress activates AMPK in cultured cells primarily by increasing cellular AMP and/or ADP. FEBS Lett. 2014;588:3361-6.
27. Fry DW, Harvey PJ, Keller PR, Elliott WL, Meade M, Trachet E, et al. Specific inhibition of cyclin-dependent kinase 4/6 by PD 0332991 and associated antitumor activity in human tumor xenografts. Mol Cancer Ther. 2004;3:1427-38.
28. Wang J, Gray NS. SnapShot: Kinase Inhibitors I. Mol Cell. 2015;58:708 e1.
29. Ikegami S, Taguchi T, Ohashi M, Oguro M, Nagano H, Mano Y. Aphidicolin prevents mitotic cell division by interfering with the activity of DNA polymerase-alpha. Nature. 1978;275:458-60.
30. Zeqiraj E, Filippi BM, Deak M, Alessi DR, van Aalten DM. Structure of the LKB1-STRAD-MO25 complex reveals an allosteric mechanism of kinase activation. Science. 2009;326:1707-11.
31. Boudeau J, Baas AF, Deak M, Morrice NA, Kieloch A, Schutkowski M, et al. MO25a/b interact with STRADa/b enhancing their ability to bind, activate and localize LKB1 in the cytoplasm. EMBO J. 2003;22:5102-14.
32. Tsou P, Zheng B, Hsu CH, Sasaki AT, Cantley LC. A fluorescent reporter of AMPK activity and cellular energy stress. Cell Metab. 2011;13:476-86.
33. Hawley SA, Ross FA, Chevtzoff C, Green KA, Evans A, Fogarty S, et al. Use of cells expressing gamma subunit variants to identify diverse mechanisms of AMPK activation. Cell Metab. 2010;11:554-65.

34. Sakamoto K, McCarthy A, Smith D, Green KA, Hardie DG, Ashworth A, et al. Deficiency of LKB1 in skeletal muscle prevents AMPK activation and glucose uptake during contraction. EMBO J. 2005;24:1810-20.
35. Sakamoto K, Zarrinpashneh E, Budas GR, Pouleur AC, Dutta A, Prescott AR, et al. Deficiency of LKB1 in heart prevents ischemia-mediated activation of AMPKalpha2 but not AMPKalpha1. Am J Physiol Endocrinol Metab. 2006;290:E780-E8.
36. Oakhill JS, Chen ZP, Scott JW, Steel R, Castelli LA, Ling N, et al. beta-Subunit myristoylation is the gatekeeper for initiating metabolic stress sensing by AMP-activated protein kinase (AMPK). Proc Natl Acad Sci USA. 2010;107:19237-41.
37. Kazgan N, Williams T, Forsberg LJ, Brenman JE. Identification of a nuclear export signal in the catalytic subunit of AMP-activated protein kinase. Mol Biol Cell. 2010;21:3433-42.
38. Suzuki A, Okamoto S, Lee S, Saito K, Shiuchi T, Minokoshi Y. Leptin stimulates fatty acid oxidation and peroxisome proliferator-activated receptor alpha gene expression in mouse C2C12 myoblasts by changing the subcellular localization of the alpha2 form of AMP-activated protein kinase. Mol Cell Biol. 2007;27:4317-27.
39. Salt IP, Celler JW, Hawley SA, Prescott A, Woods A, Carling D, et al. AMP-activated protein kinase - greater AMP dependence, and preferential nuclear localization, of complexes containing the a2 isoform. Biochem J. 1998;334:177-87.
40. Hardie DG, Schaffer BE, Brunet A. AMPK: an energy-sensing pathway with multiple inputs and outputs. Trends Cell Biol. 2016;26:190-201.
41. Evans JM, Donnelly LA, Emslie-Smith AM, Alessi DR, Morris AD. Metformin and reduced risk of cancer in diabetic patients. BMJ. 2005;330:1304-5.
42. Hardie DG. AMP-activated protein kinase: a key regulator of energy balance with many roles in human disease. J Intern Med. 2014;276:543-59.
43. Jeon SM, Hay N. The double-edged sword of AMPK signaling in cancer and its therapeutic implications. Arch Pharm Res. 2015;38:346-57.
44. Hardie DG. Molecular Pathways: Is AMPK a friend or a foe in cancer? Clin Cancer Res. 2015;21:3836-40.

45. Phoenix KN, Devarakonda CV, Fox MM, Stevens LE, Claffey KP. AMPKalpha2 suppresses murine embryonic fibroblast transformation and tumorigenesis. Genes Cancer. 2012;3:51-62.
46. Imamura K, Ogura T, Kishimoto A, Kaminishi M, Esumi H. Cell cycle regulation via p53 phosphorylation by a 5'-AMP activated protein kinase activator, 5-aminoimidazole- 4-carboxamide-1-beta-d- ribofuranoside, in a human hepatocellular carcinoma cell line. Biochem Biophys Res Commun. 2001;287:562-7.
47. Jones RG, Plas DR, Kubek S, Buzzai M, Mu J, Xu Y, et al. AMP-activated protein kinase induces a p53-dependent metabolic checkpoint. Mol Cell. 2005;18:283-93.
48. Konecny GE, Winterhoff B, Kolarova T, Qi J, Manivong K, Dering J, et al. Expression of p16 and retinoblastoma determines response to CDK4/6 inhibition in ovarian cancer. Clin Cancer Res. 2011;17:1591-602.
49. Katsumi Y, Iehara T, Miyachi M, Yagyu S, Tsubai-Shimizu S, Kikuchi K, et al. Sensitivity of malignant rhabdoid tumor cell lines to PD 0332991 is inversely correlated with p16 expression. Biochem Biophys Res Commun. 2011;413:62-8.
50. Barretina J, Caponigro G, Stransky N, Venkatesan K, Margolin AA, Kim S, et al. The Cancer Cell Line Encyclopedia enables predictive modelling of anticancer drug sensitivity. Nature. 2012;483:603-7.

# FIGURE LEGENDS

**Figure 1: Activation of AMPK by etoposide in different cell types.** (A) HeLa cells, G361 cells and immortalized mouse embryo fibroblasts (MEFs) were incubated with 30 μM etoposide for 18 hr (HeLa, G361) or with 20 μM etoposide for 2 hr (MEFs). Cell lysates were immunoprecipitated with anti-AMPK-α1 and –α2 antibodies for AMPK assay. Results are expressed relative to the mean activity (± SEM) in incubations without etoposide; results significantly different from the DMSO control by t test are indicated (HeLa and G361 cells, n = 4; MEFs, n = 3). (B) HeLa cells were incubated with increasing concentrations of etoposide, or with 10 μM A23187, for 18 hr. Upper panel: lysates were immunoprecipitated with a mixture of anti-AMPK-α1 and –α2 antibodies for AMPK assay. Results are expressed relative to the mean activity (± SEM) in incubations without etoposide or A23187 (n = 3). Results significantly different from the DMSO control by 1 way ANOVA are indicated. Equal amounts of protein from lysates from two of the three experiments were analyzed by Western blotting using anti-pSMC1, total SMC1, anti-pT172 (phospho-AMPK) and a mixture of anti-α1 and –α2 antibodies. (C) As (B), but using G361 cells.

**Figure 2:** **Etoposide activates AMPK in the nucleus**. (A) Fluorescence micrographs of HeLa cells treated for 18 hr with DMSO (control), 100 µM etoposide or 10 µM A23187. Cells were fixed, permeabilized, and stained with 4',6-diamidino-2-phenylindole (DAPI, blue), anti-pATM labelled with FITC (green) and anti-pT172 labelled with Texas red. In the right-hand images the green and red channels have been merged to assess the co-localization of pATM and pT172. Arrows show nuclei prominently labelled with anti-pT172 antibody. (B) Quantification of nuclear and cytoplasmic staining with anti-pATM and anti-pT172 in HeLa cells (left) and G361 cells (right). Using ImageJ software, the total cell area was defined, as was the area of the nuclei defined by DAPI staining. The mean fluorescence intensity in the nucleus and the cytoplasm of the etoposide- or A23187-treated cells are expressed relative to that of DMSO controls. Results are mean ± SEM (n = 10) and statistical significance of differences from DMSO controls are indicated (ns, not significant). (C) Quantification of effects of etoposide on nuclear and cytoplasmic localization of pAMPK in HEK-293 cells; analysis as in (B). Results are mean ± SEM (n = 18); ns, not significant.

**Figure 3:** **Activation of AMPK by etoposide is specific for the α1 isoform.** (A) HeLa cells were treated in triplicate with DMSO (control) or with 30 µM etoposide for 18 hr. Lysates were prepared and equal protein loadings analyzed by SDS-PAGE and Western blotting using anti-pT172 labelled with IRDye 680 (red), together with either anti-AMPK-α1 (top panel) or anti-AMPK-α2 (bottom panel) labeled with IRDye 800 (green). (B) HeLa cells were treated as in Fig. 1B, except that α1- or α2-containing complexes were immunoprecipitated separately before AMPK assay. (C), as (B), but using G361 cells; the activity of α2-containing complexes was too low to measure reliably. (D), as (B), but using A549 cells. In (B) - (D), results are mean ± SEM (n = 4 in B, n = 6-9 in C, n = 7-10 in D); statistical significnce of differences from DMSO controls are indicated.

**Figure 4: Etoposide effects on AMPK require CaMKK2 but not ATM.** (A) HeLa cells were treated with 30 μM etoposide for 18 hr with or without pre-treatment for 1 hr with 25 μM STO-609. Total AMPK was immunoprecipitated and assayed (top panel; mean ± SEM, n = 3) and Western blots of duplicate dishes of cells analyzed using various antibodies (bottom panel). (B) HeLa cells were treated with scrambled siRNA or siRNA targeted at CaMKK2 for 24 hr, prior to treatment with or without 30 μM etoposide for 18 hr; other analyses as in (A). (C) HeLa cells were treated with scrambled siRNA or siRNA targeted at CaMKK2 for 24 hr, prior to treatment with or without 10 μM A23187 for 1 hr; other analyses as in (A). (D) HeLa cells were treated with 30 μM etoposide for 18 hr with or without pre-treatment for 1 hr with 10 μM KU-55933. Total AMPK was immunoprecipitated and assayed (top panel; mean ± SEM, n = 3) and Western blots of duplicate dishes of cells analyzed using various antibodies (bottom panel).

**Figure 5: The effect of etoposide on AMPK correlates with an increase in nuclear $Ca^{2+}$.** (A) Time course of AMPK activation in HeLa cells during treatment with 30 μM etoposide; results are mean ± SEM (n = 3); values significantly different from zero time value are indicated. (B) Time course of changes in nuclear and cytoplasmic $Ca^{2+}$ in HeLa cells during treatment with 30 μM etoposide. Results (F/Fo, i.e. fluorescence as a ratio of mean fluorescence at time zero) are expressed as mean ± 95% confidence intervals (n = 12) with significant differences between etoposide-treated and control indicated at each time point.

**Figure 6: HeLa and G361 cells are protected against etoposide-induced cell death by prior AMPK activation using A23187.** (A) Parental HeLa cells (WT) or HeLa cells with CRISPR-Cas9 knockouts of AMPK-α1 (α1KO), AMPK-α2 (α2KO) or both (DKO) were treated in duplicate with 1 mM $H_2O_2$ for 10 min. Cell lysates were then analysed by Western blotting using the indicated antibodies. (B) As (A), but using G361 cells. (C) Survival of WT, single or double knockout HeLa cells assessed using MTT assays, following treatment with 10 or 30 μM etoposide for 18 hr, with or without prior treatment with 10 μM A23187 for 6 hr. Results are mean ± SEM (n = 12). Where appropriate, statistical significance is indicated by asterisks for differences between treatments with and without A23817; ns = not significant. (D) Survival of WT, single or double knockout HeLa cells assessed using clonogenic assays, following treatment with 100 or 250 nM etoposide for 18 hr, with or without prior treatment with 10 μM A23187 for 6 hr. Results are numbers of colonies counted (mean ± SEM; n = 4) expressed as a percentage of colony numbers in controls without etoposide. Where appropriate, statistical significance is indicated by asterisks for differences between treatments with and without A23817, and by daggers (†) for differences between WT and DKO; ns = not significant. (E) Phosphorylation of SMC1 in HeLa cells treated with or without different concentrations of etoposide as in (C) and (D); (F) Cell cycle arrest in WT, single or double knockout HeLa cells treated with or without 3 μM A23187 for 6 hr and then 70 ng/ml nocodazole for a further 18 hr. The cells were then fixed, stained and analyzed by flow cytometry to determine DNA content and hence cell cycle phase. Results are expressed as ratios of cells in G1:G2 phase (mean ± SEM; n = 4). Asterisks indicate the significance of differences between cells treated with and without A23187; ns, not significant.

**Figure 7: Protection against cell death using the CDK4/6 inhibitor palbociclib (PBC) correlates with its ability to cause a G1 cell cycle arrest.** (A) HeLa cells were treated with the indicated concentrations of PBC for 6 hr and then with nocodazole (70 ng/ml) for 18 hr, after which cells were fixed, stained with propidium iodide and subject to cell cycle analysis by flow cytometry. Results (mean ± SEM; n = 4) show the proportion of cells in each cell cycle phase; none of the differences between PBC treatment and controls were significant. (B) as (A), but using G361 cells; asterisks show statistically significant differences from controls without PBC. (C) Clonogenic survival of HeLa cells after treatment with or without PBC (3 µM for Hela cells; 500 nM for G361) for 6 hr, followed by treatment for a further 18 hr with vehicle (DMSO), or 100 or 250 µM etoposide. Results are numbers of colonies counted (mean ± SEM; n = 4) expressed as a percentage of survival in controls without etoposide. None of the effects of PBC were significant. (D) As (C), but using G361 cells; asterisks represent statistical significance of effects of PBC. (E) Effect of different concentrations of aphidicolin (Aph) on the cell cycle of HeLa cells, analyzed as in Figs. 7A and 7B. Asterisks indicate significant differences from the control without aphidicolin for each cell cycle phase. (F) Effect of 5 µM aphidicolin on clonogenic survival of HeLa cells treated with etoposide, analysed as in Figs 7C and 7D. Asterisks indicate significant differences from controls without etoposide.

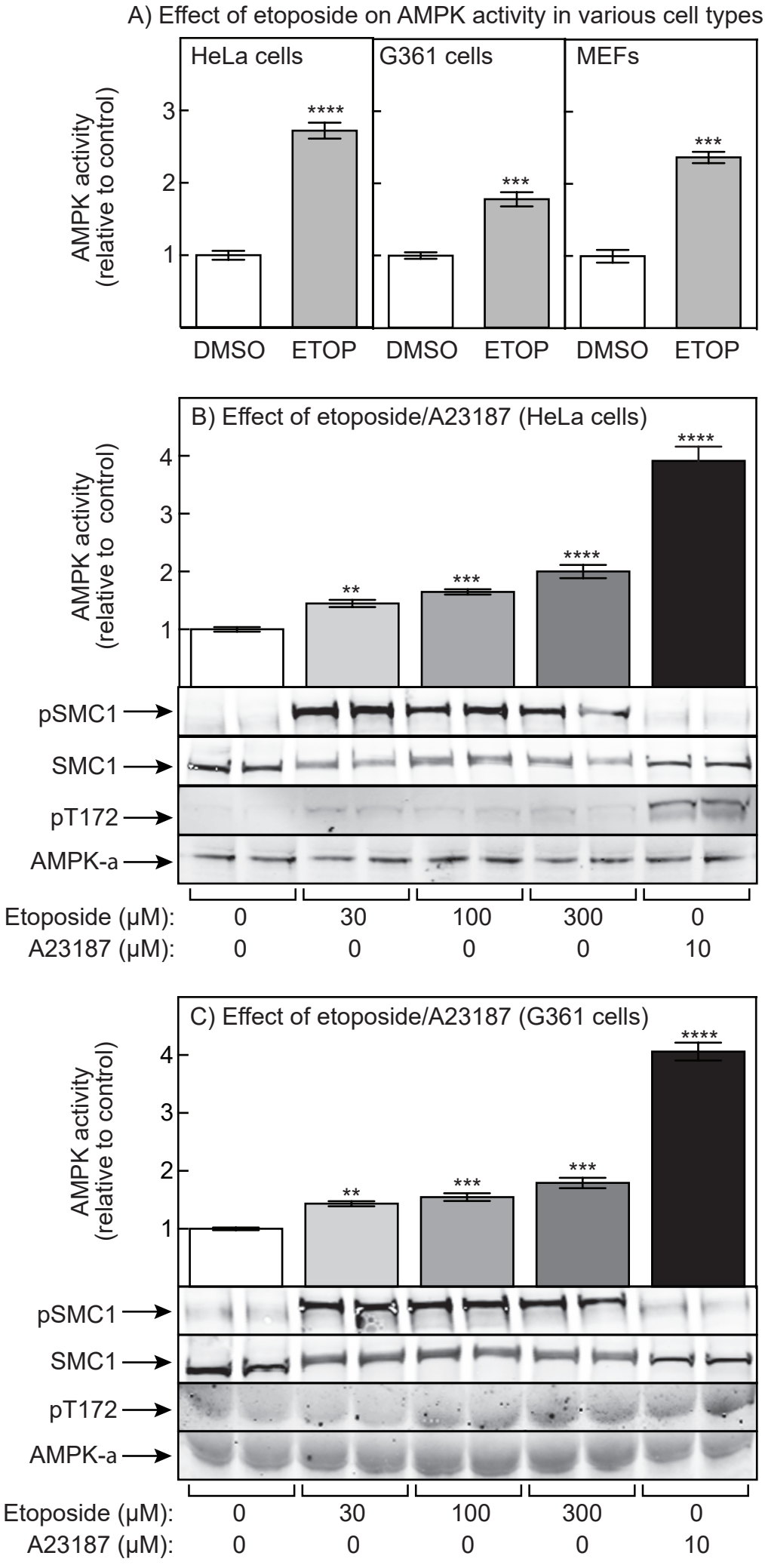
A) Effect of etoposide on AMPK activity in various cell types
HeLa cells
G361 cells
MEFs
AMPK activity (relative to control)
DMSO
ETOP
B) Effect of etoposide/A23187 (HeLa cells)
pSMC1
SMC1
pT172
AMPK-a
Etoposide (μM): 0 30 100 300 0
A23187 (μM): 0 0 0 0 10
C) Effect of etoposide/A23187 (G361 cells)

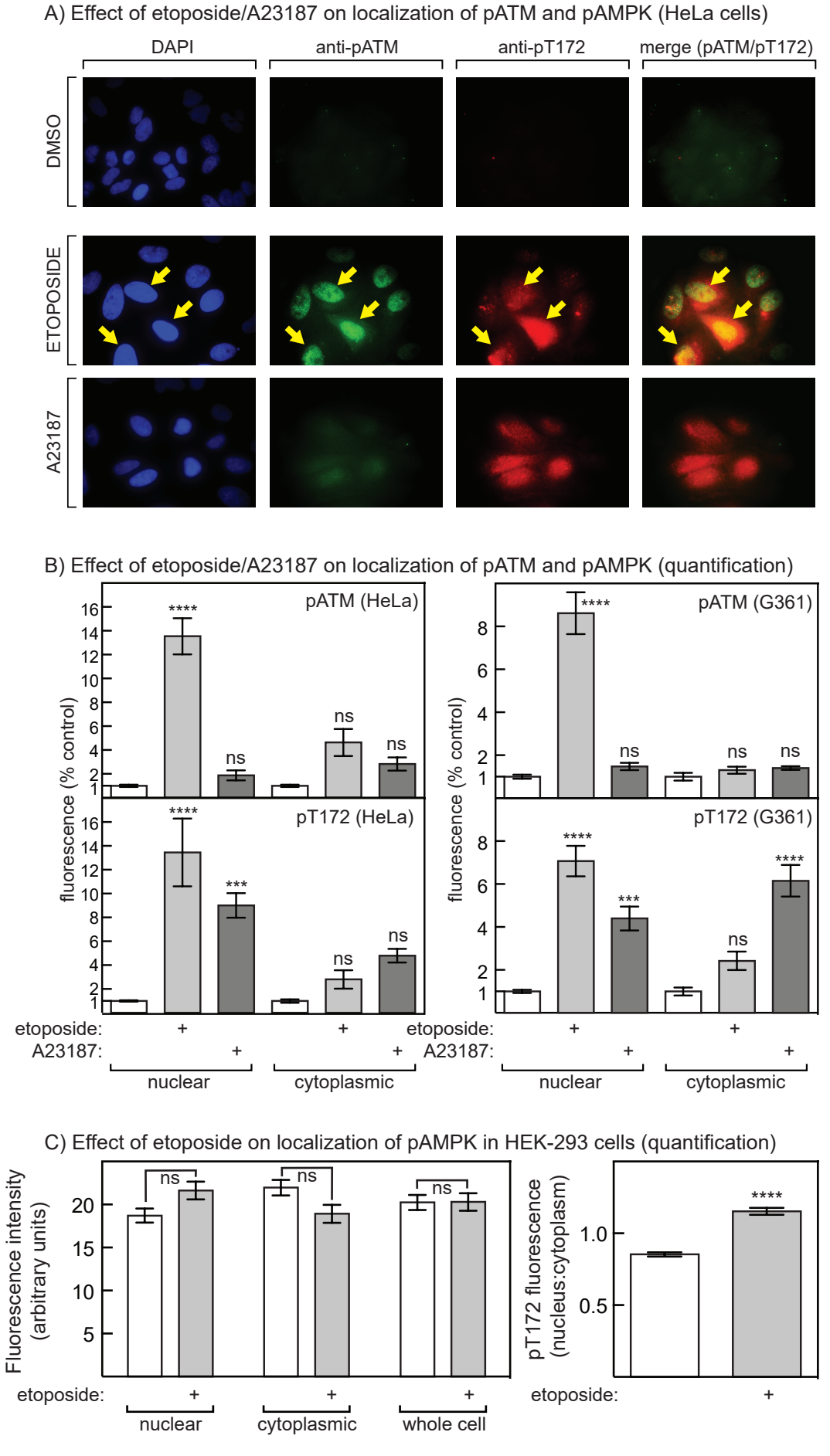
A) Effect of etoposide/A23187 on localization of pATM and pAMPK (HeLa cells)
DAPI
anti-pATM
anti-pT172
merge (pATM/pT172)
DMSO
ETOPOSIDE
A23187
B) Effect of etoposide/A23187 on localization of pATM and pAMPK (quantification)
pATM (HeLa)
pT172 (HeLa)
pATM (G361)
pT172 (G361)
fluorescence (% control)
****
***
ns
etoposide:
A23187:
nuclear
cytoplasmic
C) Effect of etoposide on localization of pAMPK in HEK-293 cells (quantification)
Fluorescence intensity (arbitrary units)
pT172 fluorescence (nucleus:cytoplasm)
whole cell

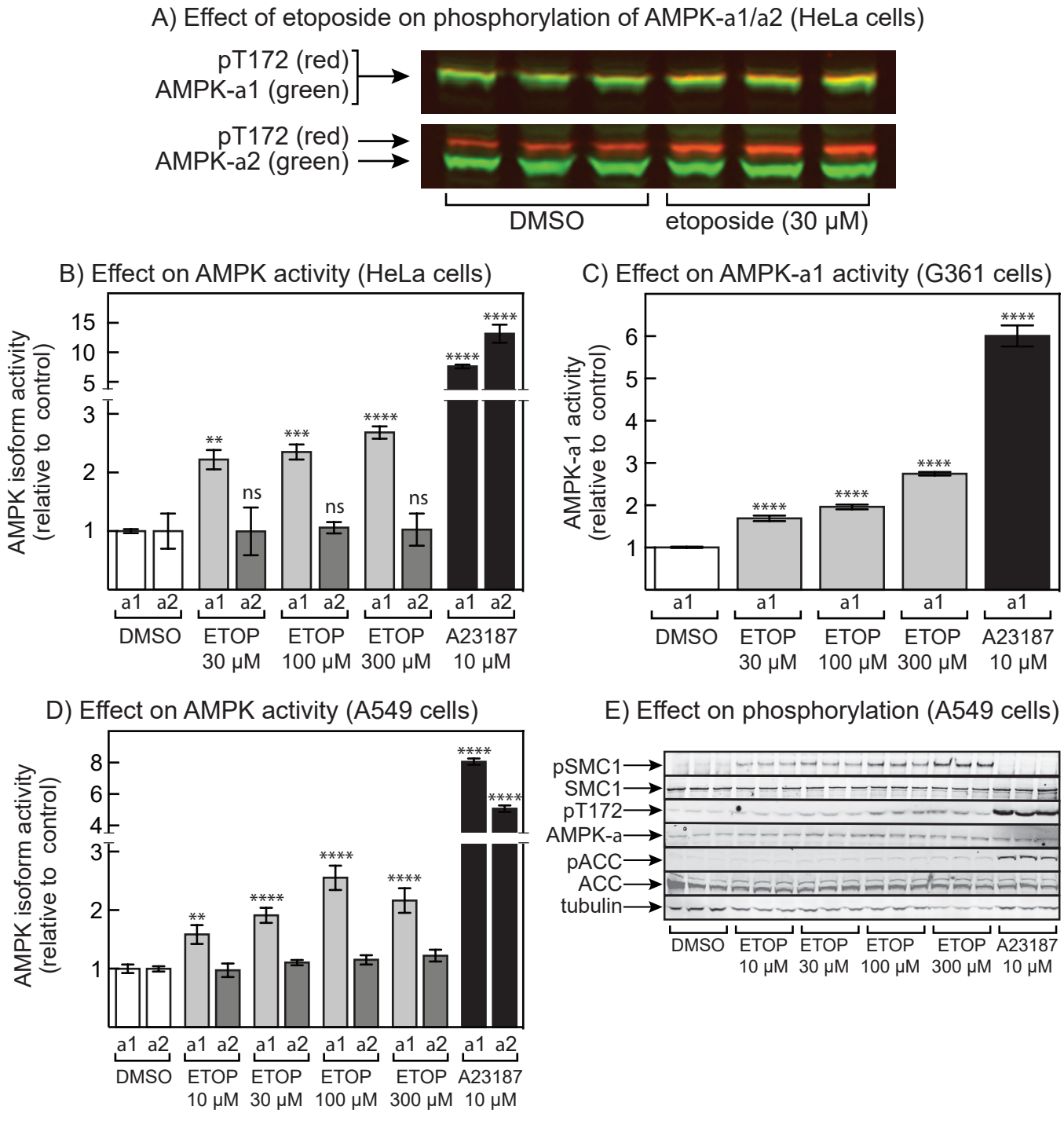
A) Effect of etoposide on phosphorylation of AMPK-a1/a2 (HeLa cells)
pT172 (red)
AMPK-a1 (green)
pT172 (red)
AMPK-a2 (green)
DMSO
etoposide (30 μM)
B) Effect on AMPK activity (HeLa cells)
AMPK isoform activity (relative to control)
15
10
5
3
2
1
**
ns
***
ns
****
ns
****
****
a1 a2 a1 a2 a1 a2 a1 a2 a1 a2
DMSO
ETOP 30 μM
ETOP 100 μM
ETOP 300 μM
A23187 10 μM
C) Effect on AMPK-a1 activity (G361 cells)
AMPK-a1 activity (relative to control)
6
5
4
3
2
1
****
****
****
****
a1 a1 a1 a1 a1
DMSO
ETOP 30 μM
ETOP 100 μM
ETOP 300 μM
A23187 10 μM
D) Effect on AMPK activity (A549 cells)
AMPK isoform activity (relative to control)
8
6
4
3
2
1
**
****
****
****
****
****
a1 a2 a1 a2 a1 a2 a1 a2 a1 a2 a1 a2
DMSO
ETOP 10 μM
ETOP 30 μM
ETOP 100 μM
ETOP 300 μM
A23187 10 μM
E) Effect on phosphorylation (A549 cells)
pSMC1
SMC1
pT172
AMPK-a
pACC
ACC
tubulin
DMSO
ETOP 10 μM
ETOP 30 μM
ETOP 100 μM
ETOP 300 μM
A23187 10 μM

A) Effect of STO-609 on etoposide activation

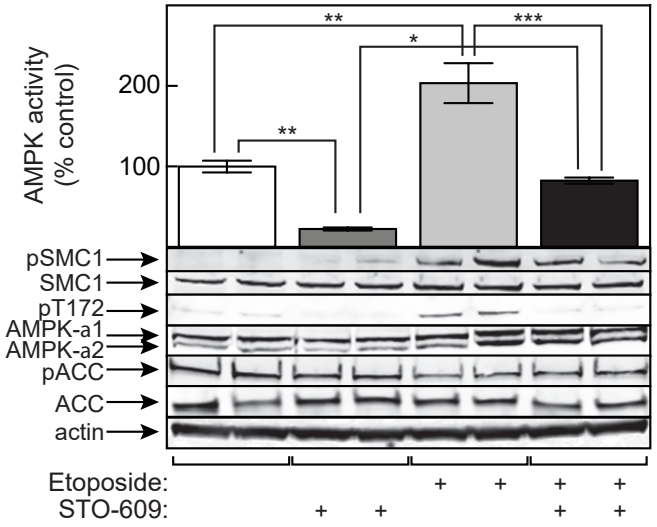


B) Effect of CaMKK2 knockdown on etoposide activation

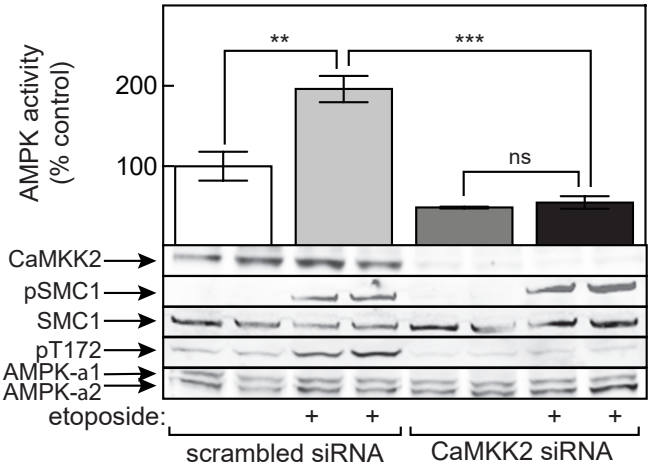


C) Effect of CaMKK2 knockdown on A23187 activation

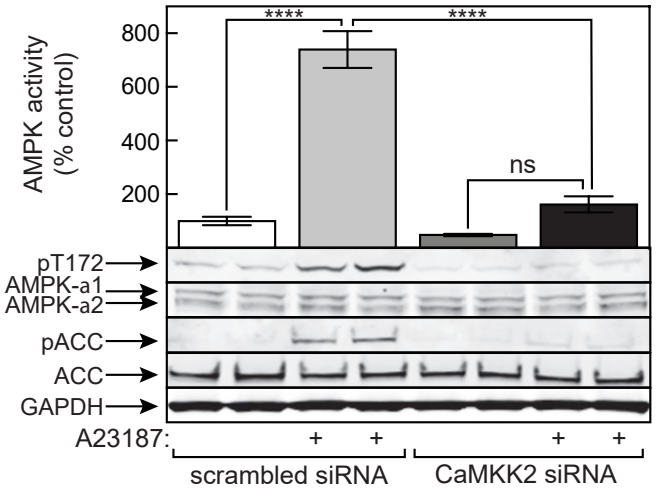


D) Effect of KU-55933 on etoposide activation

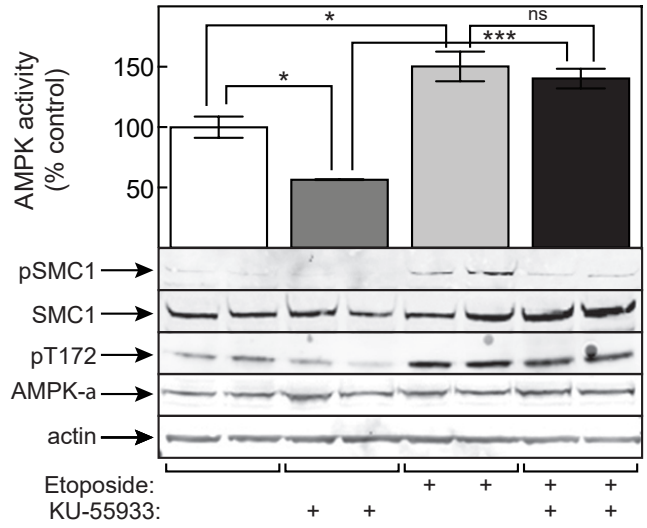

A) Time course of AMPK activation by etoposide

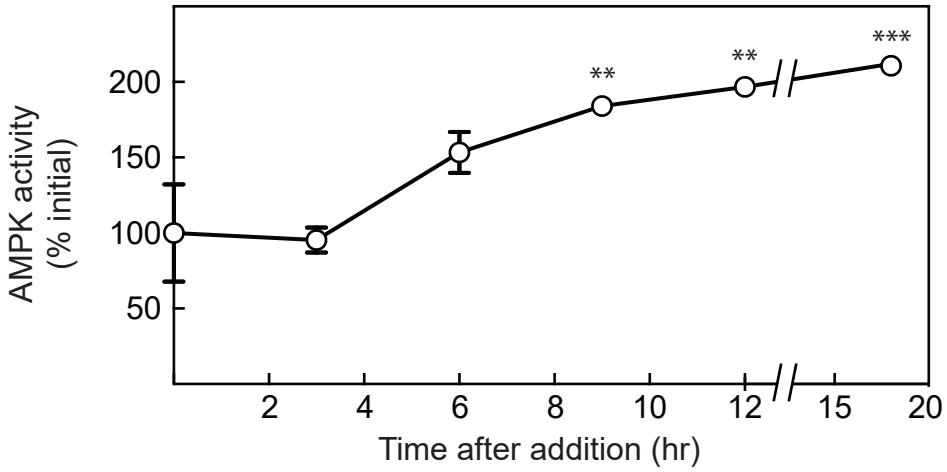


B) Nuclear/cytoplasmic [$Ca^{2+}$] after addition of etoposide

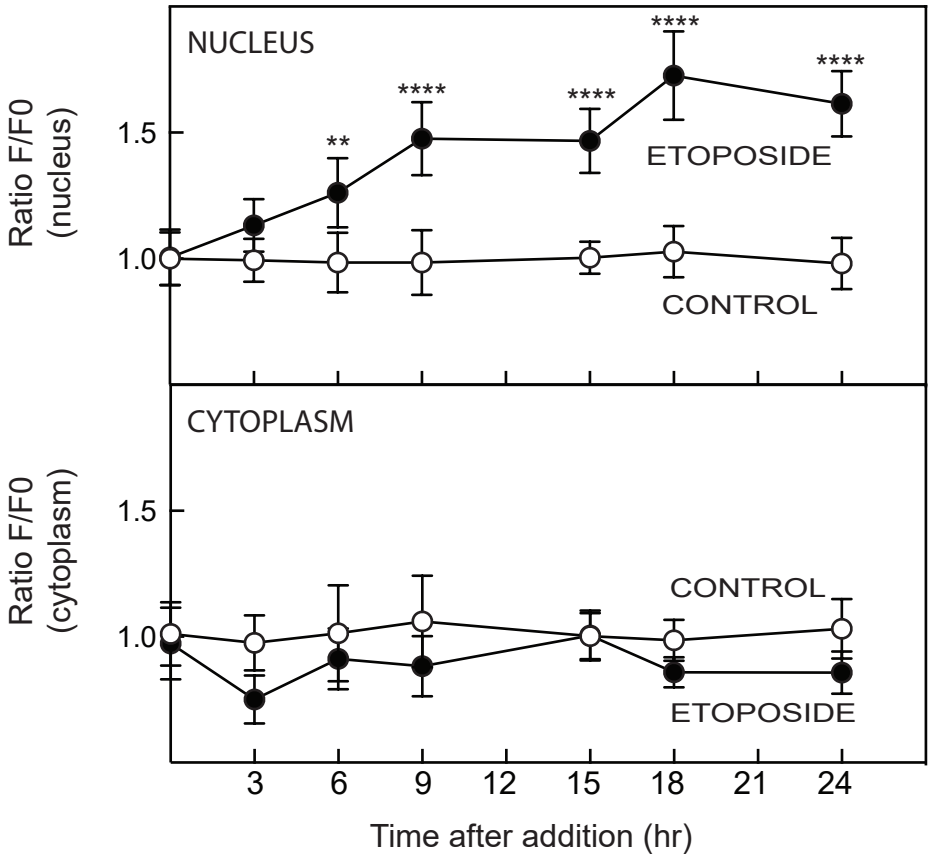

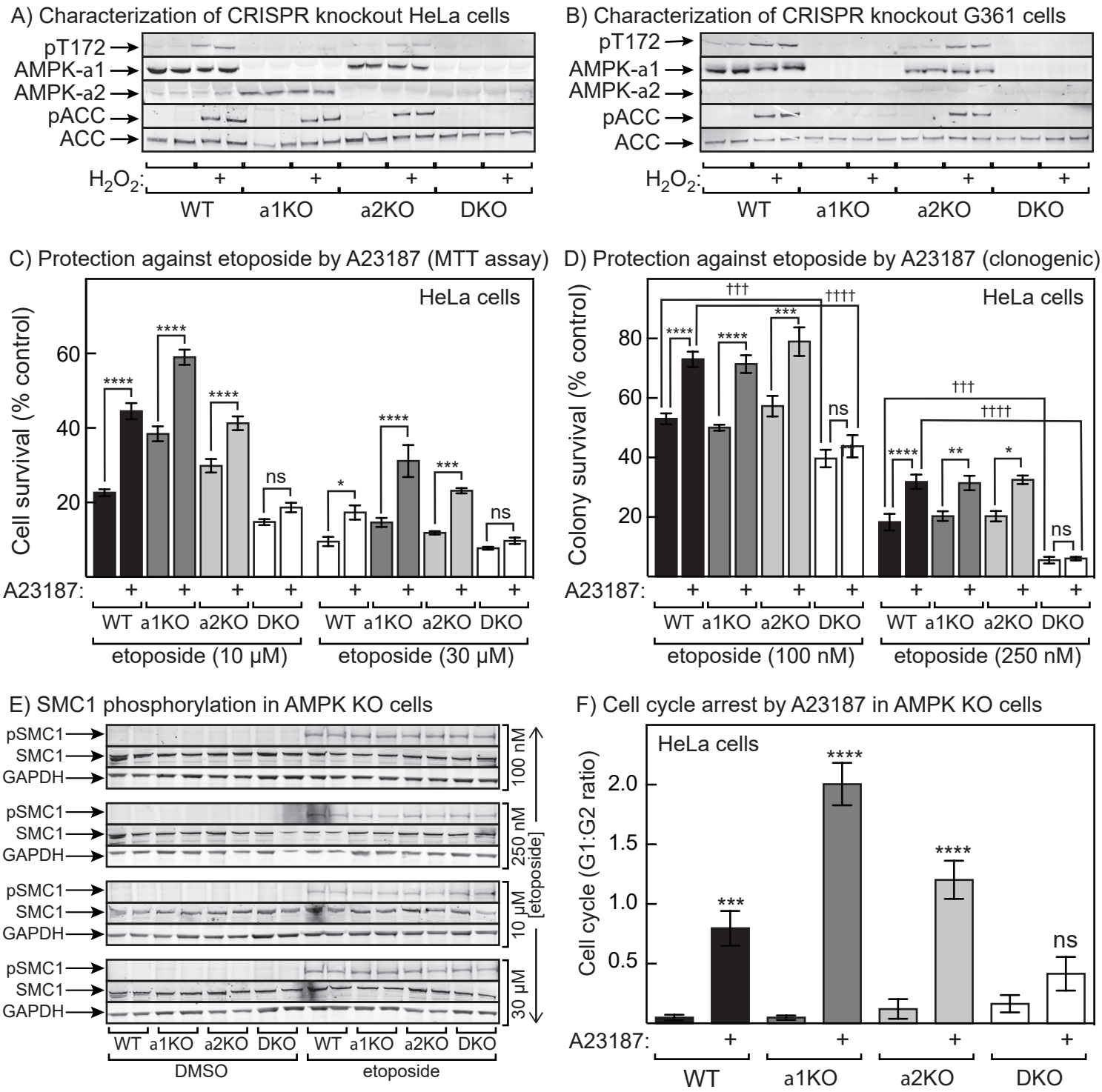
A) Characterization of CRISPR knockout HeLa cells
pT172
AMPK-a1
AMPK-a2
pACC
ACC
H2O2:
WT
a1KO
a2KO
DKO
B) Characterization of CRISPR knockout G361 cells
C) Protection against etoposide by A23187 (MTT assay)
HeLa cells
Cell survival (% control)
A23187:
etoposide (10 μM)
etoposide (30 μM)
D) Protection against etoposide by A23187 (clonogenic)
Colony survival (% control)
etoposide (100 nM)
etoposide (250 nM)
E) SMC1 phosphorylation in AMPK KO cells
pSMC1
SMC1
GAPDH
100 nM
250 nM
10 μM
30 μM
[etoposide]
DMSO
etoposide
F) Cell cycle arrest by A23187 in AMPK KO cells
Cell cycle (G1:G2 ratio)

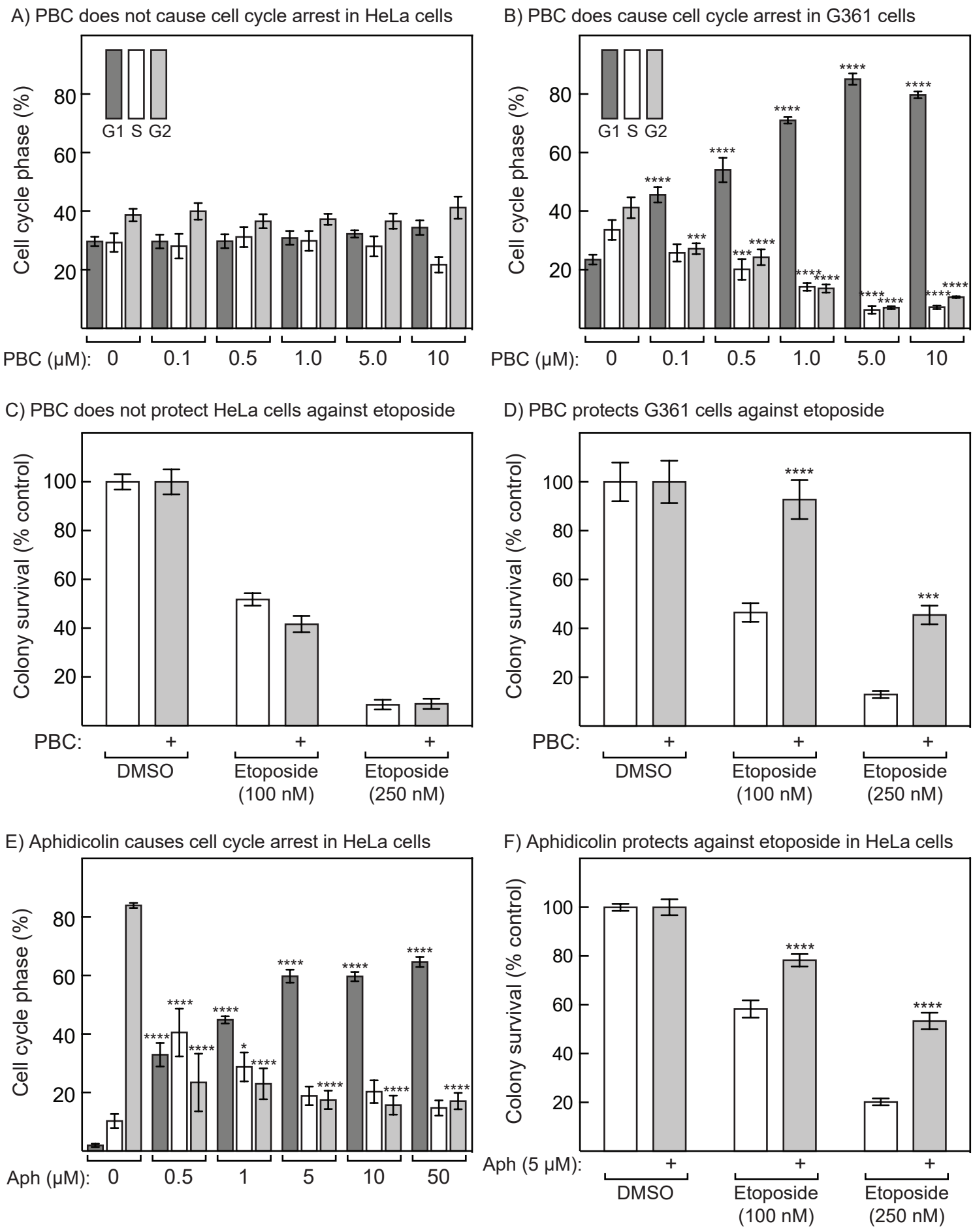
A) PBC does not cause cell cycle arrest in HeLa cells
B) PBC does cause cell cycle arrest in G361 cells
Cell cycle phase (%)
G1 S G2
PBC (μM): 0 0.1 0.5 1.0 5.0 10
C) PBC does not protect HeLa cells against etoposide
D) PBC protects G361 cells against etoposide
Colony survival (% control)
PBC:
DMSO
Etoposide (100 nM)
Etoposide (250 nM)
E) Aphidicolin causes cell cycle arrest in HeLa cells
F) Aphidicolin protects against etoposide in HeLa cells
Aph (μM): 0 0.5 1 5 10 50
Aph (5 μM):